Research Article

Simulated high frequency ray paths considering traveling ionospheric disturbances

Mariano Fagre[1,2] · Bruno S. Zossi[3,4] · Jaroslav Chum[5] · Ana G. Elias[3,4]

Received: 1 November 2019 / Accepted: 5 March 2020 / Published online: 12 March 2020

Abstract
This study presents a modified version of a classical 3-D numerical ray tracing code [originally by Jones and Stephenson (A versatile three-dimensional ray tracing computer program for radio waves in the ionosphere. Office of Telecommunications Report 75–76, US Government Printing Office, Washington, DC, 1975)], now linked to ionosphere, neutral atmosphere, Earth's magnetic field, and traveling ionospheric disturbances (TIDs) models. This method is applied to study the effect of TIDs on radio waves by simulating the waves' propagation in a disturbed ionosphere. A 3-D cubic interpolation method is implemented in the ray tracing code to solve discontinuities and guarantee the ray tracing validity and accuracy under all conditions. Changes of the ground range distance (R) and the bearing angle (σ) are assessed for various simulated ray paths. A Pedersen ray case is also shown, for which small changes of signal frequency lead to enhanced variations. The study of HF ray path variations in terms of various TIDs characteristics and under different background ionospheric conditions and transmitter locations and radiation pattern can contribute to the mitigation of TIDs effects, either helping to improve existing methods or to develop new ones. The 3-D ray tracing code described and implemented in this work may well work for this purpose.

Keywords Radio wave propagation · Traveling ionospheric disturbances · Ray tracing

1 Introduction

High frequency (HF) radio waves are used in several applications, such as long-distance communications and radar detection and tracking, using the ionosphere as a reflector in order to increase ground range. Due to the theoretical complexity of electromagnetic wave propagation through the ionosphere, which is a magnetized plasma, there still remains challenge to establish radio links as well as exact positions with radar systems. Ray tracing is commonly used to solve this problem because it allows for a calculation of the exact trajectory of radio waves, although it requires precise knowledge of the ionosphere, which is a highly variable medium [1, 2]. To its regular variations (e.g. daily and seasonal), transient disturbances are added, such as traveling ionospheric disturbances (TIDs).

In the present work, the effect of medium-scale TIDs (MSTIDs) on some characteristics of HF ray paths is analyzed. MSTIDs are often associated with the action of atmospheric gravity waves (GWs) [3, 4], with periods ranging from several minutes to less than one hour and velocities from ~ 50 to 300 m s^{-1}. TIDs effect on ray paths can result in Doppler shift of the received signal and changes of the ray trajectories, which in turn can produce apparent fluctuations on return echoes from target in radar applications, and cause coordinate registration

✉ Ana G. Elias, aelias@herrera.unt.edu.ar | [1]Consejo Nacional de Investigaciones Cientificas y Tecnicas, CONICET, Buenos Aires, Argentina. [2]Laboratorio de Telecomunicaciones, Departamento de Electricidad, Electrónica y Computación, Facultad de Ciencias Exactas y Tecnología, Universidad Nacional de Tucuman, Tucumán, Argentina. [3]Laboratorio de Fisica de La Atmosfera, Departamento de Fisica, Facultad de Ciencias Exactas y Tecnologia, Universidad Nacional de Tucuman, Tucumán, Argentina. [4]INFINOA (CONICET-UNT), Tucumán, Argentina. [5]Institute of Atmospheric Physics, Prague, Czech Republic.

SN Applied Sciences (2020) 2:615 | https://doi.org/10.1007/s42452-020-2438-4

errors for over-the-horizon radars OTHR [5]. It can also limit the performance of target detection algorithms due to the associated range and azimuth deviation that can cause a fixed target to appear to move several tens of kilometers within a few minutes [5, 6].

In this study, ray path modifications by a simulated TID are obtained using a 3-D ray tracing algorithm developed by Jones and Stephenson [7], which was modified to include the 2016 version of the International Reference Ionosphere (IRI-2016) model [8], the US Naval Research Laboratory Mass Spectrometer and Incoherent Scatter radar model (NRLMSISE-00) [9], a realistic Earth's magnetic field using the International Geomagnetic Reference Field 12th generation (IGRF-12) model [10], and Hooke's TID model [11]. In addition to the links to these models, a cubic interpolation method was implemented to guarantee continuous first derivatives in the electron density profiles [4]. A set of simulations are analyzed to demonstrate the robust performance of this ray tracing technique.

The methodology including the models used in this study is described in Sect. 2, followed by the calculation set up and obtained results description in Sects. 3 and 4. The discussion and conclusions are presented in Sects. 5 and 6 respectively.

2 Methodology

Based on Jones and Stephenson [7] algorithm, a ray tracing code shown schematically in Fig. 1 is implemented which allows to select any background ionospheric settings and TIDs characteristics under a realistic geomagnetic field. With this code the deviations induced in the ground range (R) and bearing (σ) for HF rays from a hypothetical transmitter location are obtained. R corresponds to the distance along the

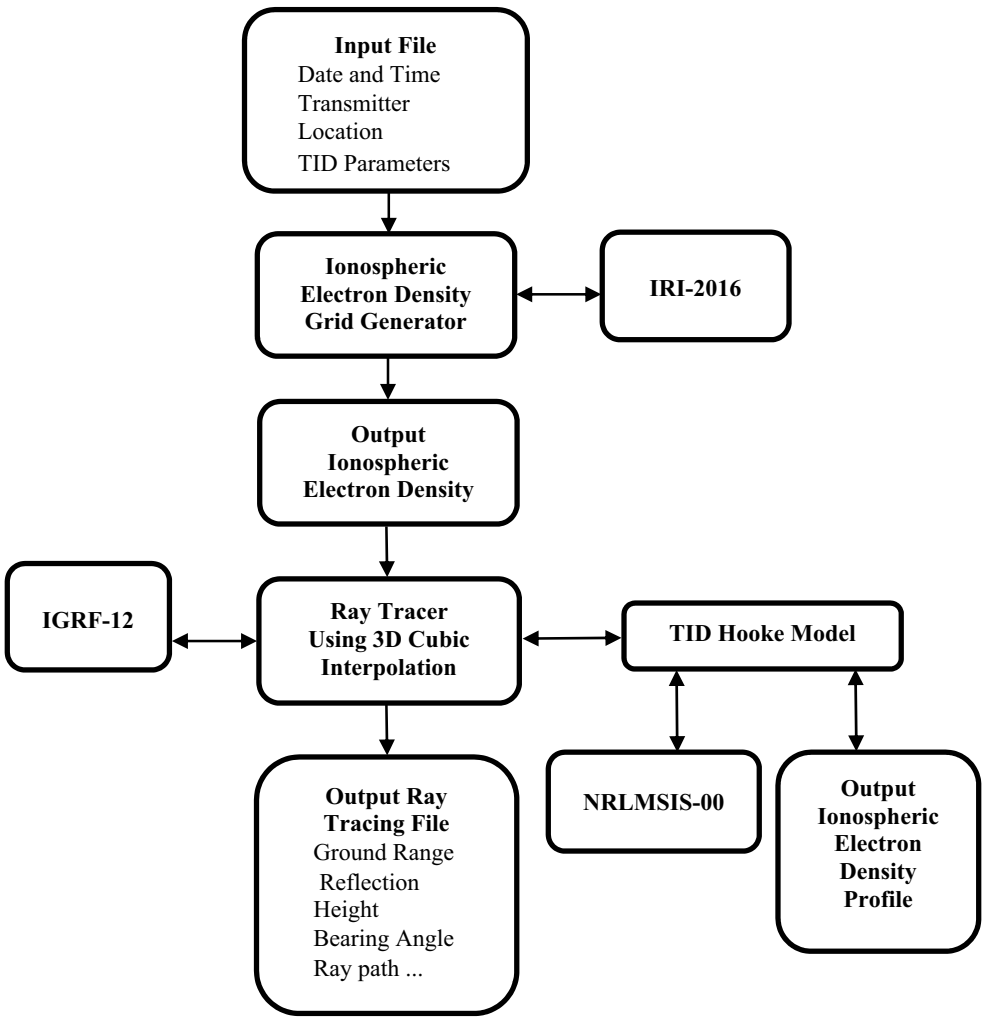

Fig. 1 Flowchart of the ray tracing code based on Jones and Stephenson [7], modified with links to several models and a cubic interpolation method

surface of Earth from the ray path origin to the point where it again reaches Earth's surface, and σ to the ray's azimuth angle of arrival measured clockwise from north. Depending on the frequency and elevation angle of the transmitted signal there are different ionospheric propagation modes reflecting from the E to the F2 layer. Ionospheric conditions can also allow Pedersen rays corresponding to reflections just below the E, F1 and F2 peaks that can reach greater distances than rays reflecting at higher altitudes. They correspond to quasi-critical propagation conditions highly sensitive to changes in the refractive index [12–14]. In fact, if the proper frequency is chosen, these rays could have infinite R for a vertically stratified ionosphere without magnetic field. Such a ray represents a singularity and can be drastically changed by any perturbation.

In the following subsections, the implemented ray tracing code, which is able to perform all propagation modes, is described.

2.1 HF signal ray tracing model

The 3-D ray tracing original code developed by Jones and Stephenson [7] was modified in order to consider variable ionospheric and neutral atmospheric conditions, and a realistic geomagnetic field configuration, linking the code to IRI-2016, NRLMSIS-00, and IGRF-12 models (Fig. 1). The code allows user-friendly modifications of these models if artificial scenarios are needed.

This ray tracing technique is based on Hamilton's equations of geometrical optics given by Haselgrove [15] in spherical coordinates.

The Hamiltonian used is given by

$$H_{(r,\theta,\varphi,k_r,k_\theta,k_\varphi)} = \frac{1}{2} * Re\left[\frac{c^2}{\omega^2}\left(k_r^2 + k_\theta^2 + k_\varphi^2\right) - n^2\right] \tag{1}$$

where n is the refractive index, c is the light velocity in free space, r, θ and φ are the spherical polar coordinates of the point at the ray path, and k_r, k_θ and k_φ are the spherical components of the HF wave vector of frequency $\omega = 2\pi f$.

We considered Appleton–Hartree equation for n in the presence of a magnetic field B, neglecting collisions, that is

$$n = \sqrt{1 - \frac{2X(1-X)}{2(1-X) - Y_T^2 \pm \sqrt{Y_T^4 + 4(1-X)^2 Y_L^2}}} \tag{2}$$

with

$$X = \frac{f_o^2}{f^2} = \frac{N_e e^2}{m\varepsilon_o (2\pi f)^2} \tag{3}$$

$$Y_T = Y\sin\theta = \frac{eB}{m(2\pi f)}\sin\theta \tag{4}$$

$$Y_L = Y\cos\theta = \frac{eB}{m(2\pi f)}\cos\theta \tag{5}$$

$$Y = \frac{eB}{m(2\pi f)} \tag{6}$$

where f_o is the plasma frequency, N_e is the electron number density, e is the electron charge, m is the electron mass, θ is the angle between the direction of the wave normal and B, T stands for transverse and L for longitudinal. The upper sign in the denominator of Eq. (2) refers to the ordinary component (o-component) and the lower sign to the extraordinary (x-component). Considering that the extraordinary wave suffers much higher absorption, only the ordinary mode will be considered.

2.2 TID model

The TID model developed by Hooke [11] was implemented as a subroutine of the main ray tracing code. It consists of a generating GW with a wave vector $\boldsymbol{k}$ of real horizontal components k and l, real vertical component m, and imaginary vertical component k_{zi}. Real components are related by the dispersion equation as follows [16]

$$m^2 = (k^2 + l^2)\left(\frac{\omega_B^2}{\omega^2} - 1\right)^2 + \frac{\left(\omega^2 - \omega_a^2\right)}{{c_s}^2} \tag{7}$$

where ω is the GW frequency, ω_B is the Brunt–Väisälä frequency, ω_a is the acoustic cutoff frequency, and c_S the speed of sound. k_{zi} is equal to $1/2H$ where H corresponds to the scale height. H, which has typical values of ~ 60 km, is given by $k_B T/Mg$, where k_B is the Boltzmann's constant, T the neutral temperature, M the mean molecular mass of the atmospheric constituents, and g the acceleration of gravity.

All the neutral parameters necessary to calculate these variables are obtained using NRLMSISE-00 [9].

Induced disturbance to electron density, N_e', below the F2 peak [17], is estimated as

$$N_e'(\vec{r}, t) = \left|N_e'\right| e^{(i\phi)} \tag{8}$$

where $|N_e'|$ is the perturbation magnitude given by

$$\left|N_e'\right| = N_e U_b(z_o) e^{\left[k_{z_i}(z - z_o)\right]} \omega^{-1} \sin(I) * \left[\left(\frac{1}{N_e}\frac{\partial N_e}{\partial z}\right)^2 + \left(\frac{k_{br}}{\sin(I)}\right)^2\right]^{\frac{1}{2}} \tag{9}$$

and ϕ the phase obtained from

$$\phi = \omega t - \boldsymbol{k} \bullet \boldsymbol{r} + tan^{-1}\left[\frac{\sin(I)}{k_{br}}\left(\frac{1}{N_e}\frac{\partial N_e}{\partial z} + k_{z_i}\right)\right] \quad (10)$$

$U_b(z_o)$ is the neutral gas velocity component associated with the gravity wave in the direction of $\boldsymbol{B}$ at the reference height z_o, I the Earth's magnetic field inclination, and k_{br} is the real part of k component parallel to $\boldsymbol{B}$ that can be calculated as the real part of $\boldsymbol{k}\cdot\boldsymbol{B}/B$.

It should also be noted that GWs can be attenuated in the F layer because of the higher air viscosity and thermal conductivity [18]. Experimentally, Chum and Podolska [19] observed an average attenuation of 0.14 dB km^{-1}. However, as a first approximation attenuation is neglected in the present work.

2.3 Interpolation method and integration

The ray tracing technique needs continuous first derivatives of N_e. This ionospheric parameter is obtained from a grid and the first derivative is calculated with a method proposed by Akyildiz [20] which guarantees the continuity required. This method known as smooth-jointed interpolation consists of a parametric curve fitting, which is cubic in each direction. It is tighter than a spline and more immune to overshoot problems between points, yet still provides continuity for the first derivative. In this way an analytic first derivative is provided.

Hamilton's equations are integrated using a Fortran subroutine which assess numerical solutions for the first-order differential equations over a specified interval and with given initial conditions applying Adams–Moulton procedure [21].

3 Calculation setup

The variables involved in the implemented ray tracing code which can be chosen independently are: frequency and elevation of the transmitted signal, date and time, transmitter location, and TIDs' parameters (z_o, $U_b(z_o)$, k, and I).

The electron density grid used by the code is generated with the IRI-2016 with a resolution of 1° × 1° in latitude and longitude, and 1 km in altitude, for the selected date and time around the transmitter location. In this case, for the undisturbed ionosphere, the quiet day January 03, 2008, at 12 LT, was considered which corresponds to summer solstice in the Southern Hemisphere and minimum solar activity level.

The hypothetical transmitter was located at 37° S, 57° W, a position chosen according to general Over the Horizon Radar, OTHR, requirements that are large unobstructed flat areas needed for the deployment of transmission and reception antennas, and coastal zones considering its general use for maritime reconnaissance. Figure 2 shows a map with the location of hypothetical transmitter and a set of paths (seen from above) indicating the azimuth range considered in this study.

To select TIDs' parameters, a GW of 240 km wavelength and 15-min period propagating northward with a velocity of ~ 260 m s^{-1} was assumed. This implies $k = 2\pi/2.4 \times 10^{-5}$ m^{-1} and $I = 0$. $U_b(z_o)$ was set to 30 m s^{-1} at $z_o = 240$ km. These values are in good agreement with values typically observed for distinct TIDs in the F2 layer by continuous Doppler sounding [22, 23]. In this case $|N_e'|/N_e$ is ~ 20% at the peak height.

4 Results

R and σ for one-way single-hop propagation were estimated first for the transmitted signal at frequencies varying between 10 and 20 MHz with a 0.2 MHz step, and with a fixed 15° elevation angle (α).

The azimuth angle of the transmitted radio waves was varied between 60° and 120° with a 5° step under the two ionospheric scenarios: unperturbed conditions and with a superposed TID. The elevation angle of 15° is typical for efficient long distance communication. In the considered frequency range, three Pedersen rays corresponding to reflections just below the E, F1 and F2 peaks are observed at frequencies ~ 10.7, ~ 13.4 and ~ 20.0 MHz, respectively. Figure 3 shows a schematic illustration with some of the ray paths obtained. The ground ranges and reflection heights of waves reflecting from the specific layers (white trajectories) increase for increasing frequency until the Pedersen ray (black trajectories) is reached.

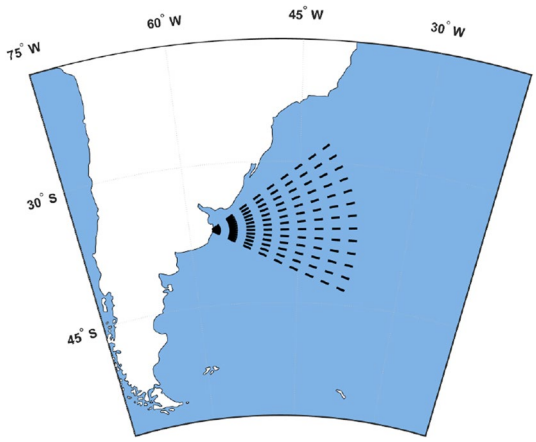

Fig. 2 Location of hypothetical transmitter, 37° S, 57° W, and ray paths with azimuth angle ranging from 60° to 120°, with a 5° step (average ground range ~ 1800 km)

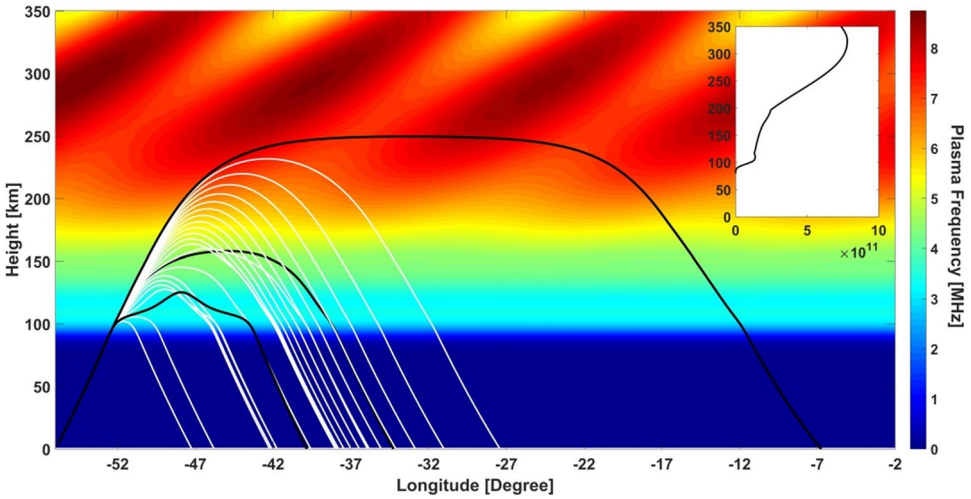

Fig. 3 Schematic illustration of ray paths for a perturbed ionosphere for the frequency range 10–20 MHz minimum and maximum frequencies, respectively) with a frequency step of 0.5 MHz and 15° elevation angle. The shortest path corresponds to 10 MHz and the longest to 20 MHz. Black ray paths correspond to Pedersen rays for ~ 10.7 (lowest black ray), ~ 13.4 (middle black ray) and ~ 20.0 MHz (highest black ray). Right corner: electron density height profile [m^{-3}] corresponding to plasma frequency shown, with E, F1 and F2 layer peaks at 110, 190 and 300 km respectively

From the 10.0–20.0 MHz frequency range, the subset 11.0–18.4 MHz is analyzed in what follows, which includes the F1 and F2 propagation mode, and the F1-layer Pedersen ray.

For the undisturbed ionosphere *R* and σ ranges between 1200 and 1800 km and 55° and 115° respectively. These ranges are obtained for α = 15°, varying the wave frequency between 11.0 and 18.4 MHz, and the azimuth angle between 60° and 120°. The only exception is the F1 region Pedersen ray at f ~ 13.4 MHz for two azimuth angles: ~ 70° and ~ 100°, where R increases markedly to 2300 km. The results of all these simulations are summarized in Fig. 4.

With the presence of TIDs, wavelike variations in both R and σ can be anticipated. This can be noticed in Fig. 5 showing both parameters in terms of time for the ionosphere disturbed by the TIDs described in Sect. 2.2. Deviations from their unperturbed value are also shown, where wavelike variations appear clearly. Larger variations are observed for higher frequencies.

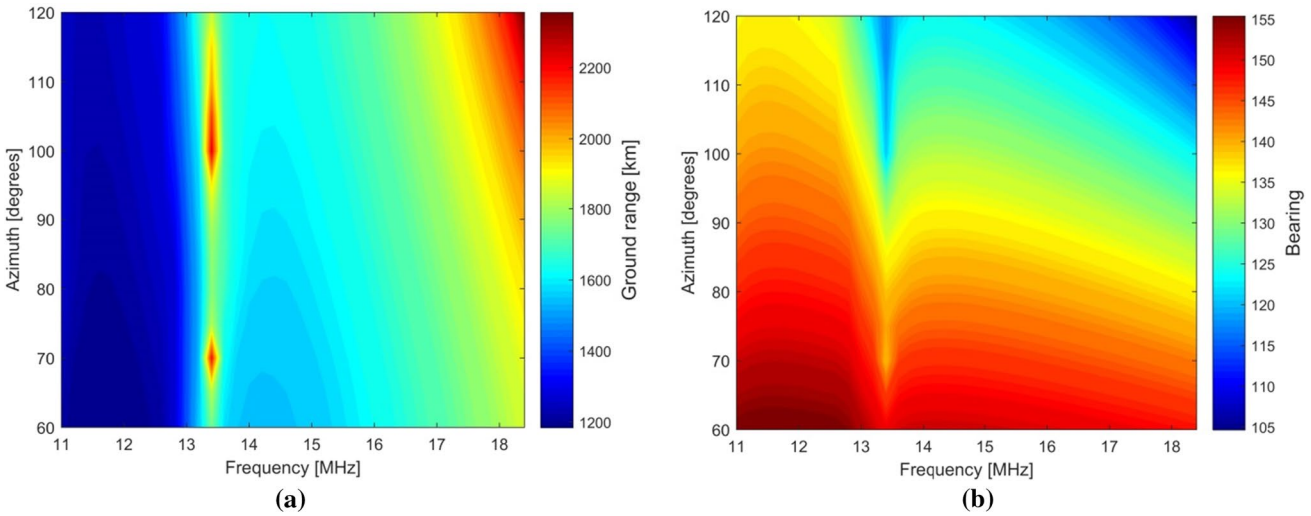

Fig. 4 **a** Ground range, R, and **b** bearing, σ, for the 11.0–18.4 MHz frequency range and 60°–120° azimuth angle range estimated with our ray tracing code for 15° elevation angle, 37° S, 57° W transmitter location, and an undisturbed background ionosphere obtained from IRI-2016 for January 03, 2008, at 12 LT (summer solstice in the Southern Hemisphere and solar minimum activity level)

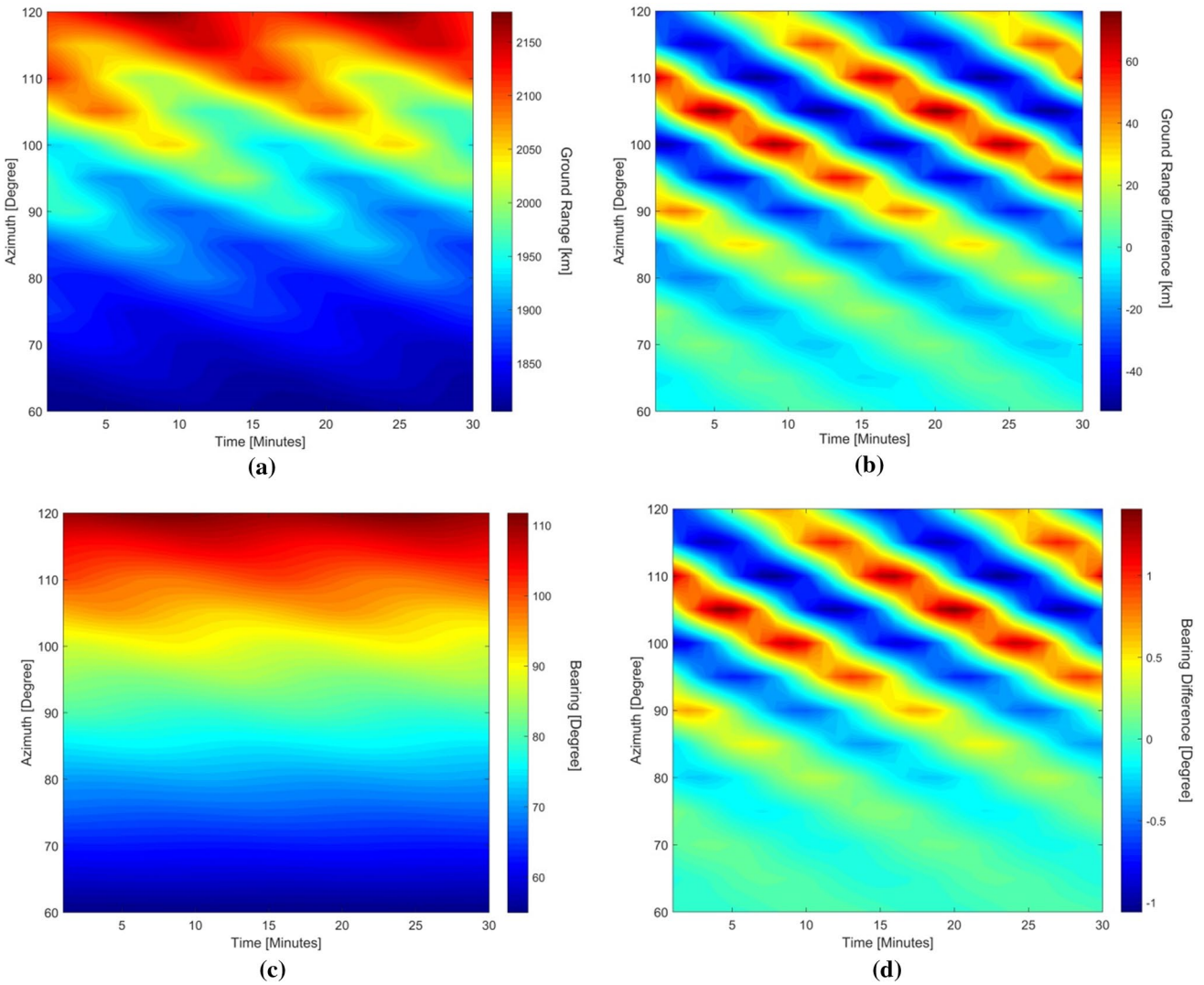

Fig. 5 **a** R and **c** σ time variation since the TID's start, and their deviation from the unperturbed values **b**, **d** for f = 18.0 MHz and α = 15°. Note the different scales. Transmitter at 37° S, 57° W. Undisturbed ionosphere obtained from IRI-2016 for January 03, 2008, at 12 LT

In the case of Pedersen ray that propagates with very small refractive index (more specifically its vertical component approaches zero), minor changes in N_e lead to significant changes in the ray trajectories that can be noticed in Fig. 6 through the time variation of R and σ.

5 Discussion

A robust ray tracing technique is implemented which can run under an ionosphere modulated by TIDs considering a realistic geomagnetic field.

Various numerical ray tracing programs have been developed so far, like IONORT by Azzarone et al. [24], PHARLAP by Cervera and Harris [17] and IONOLAB-RAY by Erdem and Arikan [25]. Even though the modular algorithm and performances are similar, in the sense that these codes and ours use the same refractive index formula and links to semi-empirical models for variables' assessment, an added-value in our case is the robust interpolation and integration method used, and the way it links to semi-empirical models which allow user-friendly modifications. For example the geomagnetic field scenarios, as done in Fagre et al. [26].

Regarding the detectable effects of TIDs, Fig. 5 shows a clear 15-min periodicity of R and σ values, together with an inclination of the perturbation pattern which is given by the GW wavelength of 240 km. In the Pedersen ray's case, shown in Fig. 6, the wavelike variations are not observed since they are screened by the strong variability for azimuths ~ 70° and ~ 100°. However, both figures correspond to specified TID's parameters used in

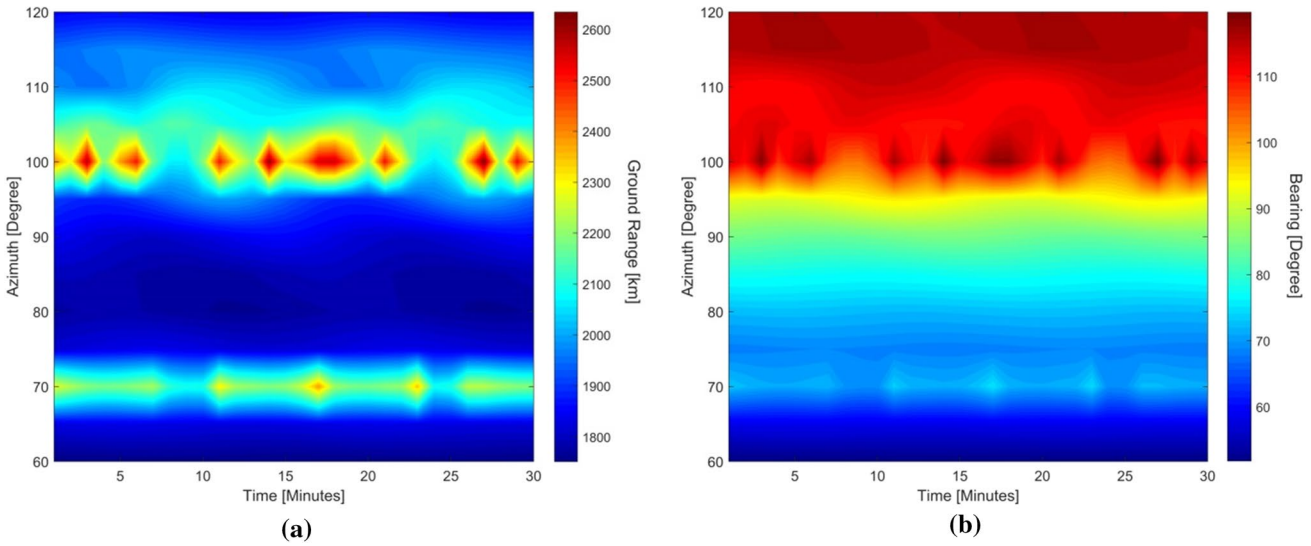

Fig. 6 **a** R and **b** time variation for f = 13.4 MHz and α = 15°, since the TID's start

this work, that strongly influence the "wavelike" characteristics of R and σ.

The wavelike structures reproduced by R and σ result in an apparent variation, or oscillation, of stationary targets, as analyzed by Nicksich et al. [27] where a solution is provided for this apparent wander of OTH targets produced by TIDs.

However, the purpose of this work is to provide a ray tracing code which works under variable and close to real conditions since it links to IRI-2016, NRLMSIS-00, and IGRF-12 models for the needed parameters. This is proved in the present work by providing the result of several simulations not only for regular ray paths but for Pedersen rays as well.

6 Conclusions

The ray path of HF signals traveling through the ionosphere depends strongly on the electron density, which in turn, varies with ionizing solar radiation conditions, season, time, location, and ionization disturbances. Considering a perturbed ionosphere with a simulated TID, *R* and σ for different ray paths were estimated from several ray paths' simulations using the ray tracing technique here proposed. Strongest effects in both parameters are observed for the frequency corresponding to the Pedersen ray, which is highly sensitive to the refractive index spatial variation. The presence of TIDs, when a radar operating frequency is too close to the maximum usable frequency that can be reflected by the ionosphere or to the Pedersen mode of propagation, can result in a loss of ionospheric reflection. In the case of the maximum usable frequency, a minimum frequency increment would bend the ray away, as in the case of the Pedersen mode due to its quasi-critical condition.

For the considered propagation conditions, TIDs effect on the Pedersen ray can be ~ 4 times larger than for other frequencies considering absolute *R* and σ values. The exact values will depend on the GW characteristics that induce the simulated TID and on the transmitter position, which determines the densities and temperatures in the ionosphere and upper atmosphere, and the Earth's magnetic field.

Modeling HF ray path variations in terms of various TIDs characteristics and under different ionospheric conditions and transmitter locations and radiation pattern can contribute to the mitigation of TIDs effects, either helping to improve existing methods or to develop new ones. The 3-D ray tracing code described and implemented in this work may well work for this purpose. It provides a computationally fast and efficient tool that can be further developed to include, for example additional options for the semi-empirical models it actually links. A natural next step will be the comparison with observational data, and the analysis of many interesting features in this field like the effect in ray paths of including ionospheric absorption in the refractive index (even though an extremely small effect) and the evaluation of TIDs effect if the Earth's magnetic field is neglected.

Acknowledgements Jaroslav Chum acknowledges the support under the Grant 18-01969S by the Czech Science Foundation. Part of this work was supported by Projects PIUNT E541 and PICT 2015-0511. Data needed to calculate ray paths were freely obtained from IRI-2016 (https://omniweb.gsfc.nasa.gov/vitmo/iri2012_vitmo.html), NRLMSISE-00 (https://ccmc.gsfc.nasa.gov/modelweb/models/nrlmsise00.php) and IGRF (https://omniweb.gsfc.nasa.gov/vitmo

/igrf_vitmo.html). The model and simulations are available from Mariano Fagre upon request (mfagre@herrera.unt.edu.ar). We would like to show our gratitude to Dr. L. J. Nickisch from Norwest Research Associates (NWRA) for all his help in the implementation of the Hooke model in our code and also for his useful and enriching comments.

Funding This study was funded by Grant 18-01969S of the Czech Science Foundation, and Projects PIUNT E541 and PICT 2015-0511 from Argentina.

Compliance with ethical standards

Conflict of interest The authors declare that they have no conflict of interest.

References

1. Davies K (1965) Ionospheric radio propagation. U. S. Department of Commerce, National Bureau of Standards, Monograph 80, Washington, DC
2. Rishbeth H, Garriott OK (1969) Introduction to ionospheric physics. Academic Press, New York
3. Hocke K, Schlegel K (1996) A review of atmospheric gravity waves and travelling ionospheric disturbances: 1982–1995. Ann Geophys 14:917–940
4. Nickisch LJ, Fridman S, Hausman M, San Antonio GS (2016) Feasibility study for reconstructing the spatial–temporal structure of TIDs from high-resolution backscatter ionograms. Radio Sci 51:443–453
5. Reinisch B, Galkin I, Belehaki A et al (2018) Pilot ionosonde network for identification of traveling ionospheric disturbances. Radio Sci 53:365–378
6. Nickisch LJ, Hausman MA, Fridman SV (2006) Range rate—Doppler correlation for HF propagation in traveling ionospheric disturbance environments. Radio Sci 41:RS5–RS39
7. Jones RM, Stephenson JJ (1975) A versatile three-dimensional ray tracing computer program for radio waves in the ionosphere. Office of Telecommunications Report 75–76, US Government Printing Office, Washington, DC
8. Bilitza D, Altadill D, Truhlik V, Shubin V, Galkin I, Reinisch B, Huang X (2017) International reference ionosphere 2016: from ionospheric climate to real-time weather predictions. Space Weather 15:418–429
9. Picone JM, Hedin AE, Drob DP, Aikin AC (2002) NRLMSISE-00 empirical model of the atmosphere: statistical comparisons and scientific issues. J Geophys Res 107(A12):1468
10. Thebault E, Finlay CC, Beggan C, Alken P, Aubert J et al (2015) International geomagnetic reference field: the 12th generation. Earth Planets Space 67:79
11. Hooke WH (1968) Ionospheric irregularities produced by internal atmospheric gravity waves. J Atmos Terr Phys 30:795–823
12. Tinin MV (1981) Asymptotic methods in the determination of the arrival angles of the Pedersen ray and the skip distance in a horizontally inhomogeneous atmosphere. Radiophys Quantum Electron 24:814–819
13. Kulizhskii AV, Tinin MV (1993) Average Pedersen-ray intensity in randomly inhomogeneous ionosphere. Radiophys Quantum Electron 36:253–255
14. Erukhimov LM, Uryadov VP, Cherkashin YN, Eremenko VA, Ivanov VA, Ryabova NV, Shumaev VV (1997) Pedersen mode ducting in a randomly stratified ionosphere. Waves Random Media 7:531–544
15. Haselgrove J (1955) Ray theory and a new method for raytracing. Physics of the Ionosphere, Physical Society, London, pp 355–364
16. Hines CO (1960) Internal atmospheric gravity waves at ionospheric heights. Can J Phys 38:1441–1481
17. Cervera MA, Harris TJ (2014) Modeling ionospheric disturbance features in quasi-vertically incident ionograms using 3-D magnetoionic ray tracing and atmospheric gravity waves. J Geophys Res 119:431–440
18. Vadas SL, Fritts DC (2005) Thermospheric responses to gravity waves: influences of increasing viscosity and thermal diffusivity. J Geophys Res 110:D15103
19. Chum J, Podolská K (2018) 3D analysis of GW propagation in the ionosphere. Geophys Res Lett 45:11,562–11,571
20. Akyildiz Y (1994) Parametric curve fitting: an alternative to Lagrange interpolation and splines. Comput Phys 8:722–729
21. Lastman GJ (1964) Solution of N simultaneous first-order differential equations by either the Runge–Kutta method or by the Adams–Moulton method with a Runge–Kutta starter, using partial double-precision arithmetic, D2 UTEX RKAMSUB, The University of Texas
22. Chum J, Bonomi FAM, Fišer J, Cabrera MA, Ezquer RG, Burešová D, Laštovička J et al (2014) Propagation of gravity waves and spread F in the low-latitude ionosphere over Tucumán, Argentina, by continuous Doppler sounding: first results. J Geophys Res 119:6954–6965
23. Fišer J, Chum J, Liu JY (2017) Medium-scale traveling ionospheric disturbances over Taiwan observed with HF Doppler sounding. Earth Planets Space 69:131
24. Azzarone A, Bianchi C, Pezzopane M, Pietrella M, Scotto C, Settimi A (2012) IONORT: a windows software tool to calculate the HF ray tracing in the ionosphere. Comput Geosci 42:57–63
25. Erdem E, Arikan F (2017) IONOLAB-RAY: a wave propagation algorithm for anisotropic and inhomogeneous ionosphere. Turk J Electr Eng Comput Sci 25:1712–1723
26. Fagre M, Zossi BS, Yigit E, Amit H, Elias AG (2020) High frequency sky wave propagation during geomagnetic field reversals. Stud Geophys Geod 64:130–142
27. Nickisch LJ, Hausman MA, Fridman S (2007) Traveling ionospheric disturbance mitigation for OTH radar. In: 2007 IEEE radar conference, pp 362–366